Jpn. J. Appl. Phys. Vol. 40 (2001) pp. 4045–4050
Part 1, No. 6A, June 2001

Ultra Short Two-Section Vertical Directional Coupler Switches with High Extinction Ratios

Sung-Chan CHO, Boo-Gyoun KIM[1], Yong MOON[1] and Ali SHAKOURI[2]

Optical Packet Switch Team, ETRI, Taejon 305-350, Korea
[1]*School of Electronic Engineering, Soongsil University, Seoul 156-743, Korea*
[2]*Baskin School of Engineering, University of California, Santa Cruz, CA 95064, USA*

(Received November 8, 2000; accepted for publication March 16, 2001)

We show that both cross and bar states with high extinction ratios larger than 30 dB can be achieved at the same end of ultra short fused vertical directional coupler switches (FVCSs) with two sections by changing the refractive indices of cores and inner cladding layer less than 1%. The improvement of extinction ratios for various combinations of the refractive indices in a two-section FVCS is studied using the improved coupled theory and beam propagation method. Design guidelines to achieve high extinction ratios with large tolerances are presented.

KEYWORDS: asymmetric coupler, extinction ratio, optical switch, fused vertical directional coupler, wafer fusion

1. Introduction

Major requirements for optical packet switching elements are low loss, scalability, low polarization dependence, and high extinction ratios. Recently, a novel fused vertical coupler (FVC) with a very short coupling length of 62 μm was demonstrated.[1)] Since the technique of wafer fusion can be used to combine waveguides fabricated on two different substrates into three-dimensional structures, the problem of the two vertical waveguide separation can be solved. In addition, application of a bias at the fused layers will allow a change of mode overlap integral for switching purposes.[1)]

Ultra short directional couplers have an inherent limitation in their cross state extinction ratio due to non-orthogonality of individual waveguide modes. One can improve the extinction ratio for the cross state by using slight asymmetry in the structure.[2)] This comes, however, at the expense of poorer bar state extinction ratios. For the application of FVCs as switching elements, both cross and bar states should have high extinction ratios. One can achieve the bar state with high extinction ratios larger than 30 dB by employing two-section structures with a proper asymmetry in the first section and a symmetric second section. The core refractive indices for the waveguides in section 2 should be equal to the core index of the waveguide in section 1 in which the power is not launched. In these structures the bar state with high extinction ratios larger than 30 dB can be achieved at the ends of section 2.[3)]

We show that both cross and bar states with high extinction ratios larger than 30 dB can be achieved in ultra short ($< 100\,\mu$m) fused vertical directional coupler switches (FVCSs) with two sections by modifying the refractive indices of cores and inner cladding layers by an amount less than 1%. Transfer matrix method and the improved coupled mode theory (ICMT) are used to analyze these structures and the results are compared with those of the 2D finite difference beam propagation method (BPM). In addition, the design guidelines to achieve high extinction ratios with large tolerances are presented.

This paper is organized as follows. In §2, the improved coupled mode theory (ICMT) and the transfer matrix method are briefly described for multisection vertical directional couplers. Section 3 gives the design procedure and examples for ultra short fused vertical directional coupler switches with two sections which have both cross and bar states with high extinction ratios larger than 30 dB. Also, the design guidelines to achieve high extinction ratios with large tolerances are presented. Finally, conclusions are given in §4.

2. Improved Coupled Mode Theory and Transfer Matrix Method in Multisection Vertical Directional Couplers

The improved coupled mode equations in the ith segment of a two-section vertical directional coupler shown in Fig. 1 are given by[4)]

$$\frac{d}{dz}a^{(i)}(z) = -i\gamma_{(a)}^{(i)}a^{(i)}(z) - ik_{ab}^{(i)}b^{(i)}(z) \tag{1}$$

$$\frac{d}{dz}b^{(i)}(z) = -ik_{ba}^{(i)}a^{(i)}(z) - i\gamma_{(b)}^{(i)}b^{(i)}(z) \tag{2}$$

where

$$\gamma_{(a)}^{(i)} = \beta_a^{(i)} + \frac{K_{aa}^{(i)} - C_{(i)}K_{ba}^{(i)}}{1 - C_{(i)}^2},$$

$$\gamma_{(b)}^{(i)} = \beta_b^{(i)} + \frac{K_{bb}^{(i)} - C_{(i)}K_{ab}^{(i)}}{1 - C_{(i)}^2},$$

$$k_{ab}^{(i)} = \frac{K_{ab}^{(i)} - C_{(i)}K_{bb}^{(i)}}{1 - C_{(i)}^2},$$

$$k_{ba}^{(i)} = \frac{K_{ba}^{(i)} - C_{(i)}K_{aa}^{(i)}}{1 - C_{(i)}^2},$$

$$k_{ab}^{(i)} = \frac{\omega}{4}\iint \Delta\varepsilon_{(q)}^{(i)}[\boldsymbol{E}_{t,a}^{(i)} \cdot \boldsymbol{E}_{t,b}^{(i)} - \boldsymbol{E}_{z,a}^{(i)} \cdot \boldsymbol{E}_{z,b}^{(i)}]dxdy$$

$$C_{(i)} = \frac{C_{ab}^{(i)} + C_{ba}^{(i)}}{2},$$

$$C_{ab}^{(i)} = \frac{1}{2}\iint \boldsymbol{E}_{t,b}^{(i)} \times \boldsymbol{H}_{t,a}^{(i)} \cdot \hat{z}dxdy,$$

$$C_{ba}^{(i)} = \frac{1}{2}\iint \boldsymbol{E}_{t,a}^{(i)} \times \boldsymbol{H}_{t,b}^{(i)} \cdot \hat{z}dxdy,$$

$\boldsymbol{E}_{t,a}^{(i)}$ and $\boldsymbol{H}_{t,a}^{(i)}$ and $\boldsymbol{E}_{t,b}^{(i)}$ and $\boldsymbol{H}_{t,b}^{(i)}$ are the transverse electric and magnetic fields of waveguides A and B in the ith section, respectively. And $a^{(i)}(z)$ and $b^{(i)}(z)$ are the mode amplitudes of waveguides A and B in the ith section, respectively.

The mode amplitudes at the end of section 2 of waveguides A and B, $a^{(2)}(L)$ and $b^{(2)}(L)$, can be expressed by the transfer matrix and are related to the mode amplitudes of waveguides A and B at the input of section 1, $a^{(1)}(0)$ and $b^{(1)}(0)$, as follows:

$$\begin{bmatrix} a^{(2)}(L) \\ b^{(2)}(L) \end{bmatrix} = T^{(2)}T^{(1)} \exp\left[-i(\phi^{(1)} + \phi^{(2)})\right] \begin{bmatrix} a^{(1)}(0) \\ b^{(1)}(0) \end{bmatrix} \quad (3)$$

where the transfer matrix in the ith section is given by

$$T^{(i)} = \begin{bmatrix} \cos\psi^{(i)}l^{(i)} + i\dfrac{\Delta^{(i)}}{\psi^{(i)}}\sin\psi^{(i)}l^{(i)} & -i\dfrac{k_{ab}^{(i)}}{\psi^{(i)}}\sin\psi^{(i)}l^{(i)} \\ -i\dfrac{k_{ba}^{(i)}}{\psi^{(i)}}\sin\psi^{(i)}l^{(i)} & \cos\psi^{(i)}l^{(i)} - i\dfrac{\Delta^{(i)}}{\psi^{(i)}}\sin\psi^{(i)}l^{(i)} \end{bmatrix} \quad (4)$$

where

$$\Delta^{(i)} = \frac{\gamma_b^{(i)} - \gamma_a^{(i)}}{2},$$

$$\psi^{(i)} = \sqrt{\Delta^{(i)2} + k_{ab}^{(i)}k_{ba}^{(i)}},$$

and $l^{(i)}$ is the length of each section.

The output power at the end of each section for waveguides A and B, $P_a^{(i)}$ and $P_b^{(i)}$, are given by

$$P_a^{(i)} = \mathrm{Re}\lfloor(a^{(i)}(l^{(i)}) + C_{ab}^{(i)}b^{(i)}(l^{(i)}))(a^{*(i)}(l^{(i)}) + C_{ba}^{*(i)}b^{*(i)}(l^{(i)}))\rfloor \quad (5)$$

$$P_b^{(i)} = \mathrm{Re}\lfloor(C_{ba}^{(i)}a^{(i)}(l^{(i)}) + b^{(i)}(l^{(i)}))(C_{ba}^{*(i)}a^{*(i)}(l^{(i)}) + b^{*(i)}(l^{(i)}))\rfloor. \quad (6)$$

3. Simulation Results and Design Guidelines

Figure 1(a) shows the FVCS with separated input and output waveguides. Since the two-dimensional index profile of an FVCS could be reduced to one dimension using the effective index method, the coupling length and the extinction ratio for TE mode are calculated in the slab waveguide geometry to obtain the design guidelines. The schematic diagram of the one-dimensional index profile in the straight interaction region of vertical directional coupler switches with two sections is shown in Fig. 1(b). The parameter values used in our analysis are $n_{ca} = n_{cb} = 3.17$, $n_b(1) = n_b(2) = 3.37$, $d_a = d_b = 0.5\,\mu$m, and the wavelength is $1.55\,\mu$m. The results for the TE mode are presented. The results of the TM mode are similar to those of the TE mode. Assuming that the power is incident into the waveguide A, without the loss of generality, the extinction ratio of cross and bar states of the section i is defined as $P_b^{(i)}/P_a^{(i)}$ and $P_a^{(i)}/P_b^{(i)}$, respectively, where $P_a^{(i)}$ and $P_b^{(i)}$ are the guided mode powers at the end of each section of waveguides A and B, respectively.

Both cross and bar states can be achieved at the end of a device if we match the twice coupling length of the bar state to the triple coupling length of the cross state by changing the refractive index of inner cladding layers. High extinction ratios for the cross state is achieved by controlling the asymmetry of refractive indices of cores for $n_a(1) = n_a(2)$ and $n_b(1) = n_b(2)$. Also, one can achieve high extinction ratios for the bar state using the optimum asymmetry of refractive indices of cores in section 1 for $n_b(1) = n_a(2) = n_b(2)$.[3] That is, switching operation is achieved by changing the refractive index of the inner cladding layer. And high extinction ratios for both cross and bar states are achieved by the asymmetry of refractive indices of cores.

The procedure for the design of ultra short fused vertical directional coupler switches is as follows:

1. Calculate the device length ($L = l_{c,1} + l_{c,2}$) of a bar state as a function of the refractive index of the inner cladding layer for $n_a(1)$ at which the maximum extinction ratio occurs when $n_b(1) = n_a(2) = n_b(2) = 3.37$ in two-section fused vertical couplers.
2. Calculate the device length ($L = 3l_{c,\mathrm{cross}}$) of a cross state as a function of the refractive index of the inner cladding layer for $n_a(1) = n_a(2)$ at which the maximum extinction ratio occurs when $n_b(1) = n_b(2) = 3.37$.
3. Find the range of the difference of refractive indices of inner cladding layers less than 1% between bar and cross states.
4. Find the range of the optimum asymmetry of refractive indices of cores less than 1% within the range of finding through procedure 3.
5. Based on the results of the above procedures, determine the refractive index of the inner cladding layer providing the same device length for bar and cross states and control the asymmetry of refractive indices of cores to achieve the high extinction ratios larger than 30 dB.

Figure 2 shows the device length for bar and cross states as a function of the refractive index of the inner cladding layer when the inner cladding layer thickness is $0.6\,\mu$m. In order to achieve high extinction ratios larger than 30 dB, the index of waveguide A in section one [$n_a(1)$] has been optimized. One can see that the refractive index change of the inner cladding layer for a switching operation decreases as the refractive index of the inner cladding layer increases. Also, the results of ICMT agree very well with those of BPM.

Figure 3 gives the detail of Fig. 2 showing the range in refractive index of the inner cladding layer for a switching operation with the change of refractive indices of the inner cladding layer and cores less than 1% ($= 0.03$). The change of refractive index of the inner cladding layer for a switching

operation is denoted by $\Delta n_{ci} = n_{ci,\mathrm{cross}} - n_{ci,\mathrm{bar}}$. The optimum asymmetry of refractive indices of two cores in section 1 at which the maximum extinction ratio occurs is denoted by $\Delta n_{\mathrm{asy}} = n_b - n_a$. Also, one can see that the asymmetry of the refractive indices of two cores in section 1 (equal to the change of refractive index of core A) increases as the refractive index of the inner cladding layer increases (see Fig. 3 inset). The change of the inner cladding layer refractive index for a switching operation is larger than 0.03 for the refractive index of the inner cladding layer less than 3.21. And the asymmetry of the refractive indices of two cores is larger than 0.03 for the inner cladding layer refractive index larger than 3.25. Thus, FVCSs must be designed in the range of the refractive index of the inner cladding layer from 3.21 to 3.25.

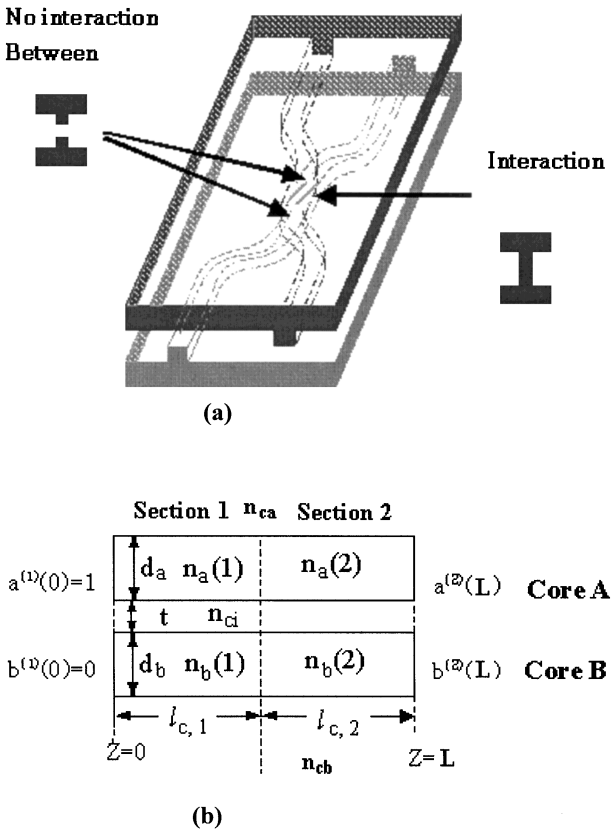

Fig. 1. (a) Fused vertical coupler switches with separated input and output waveguides. (b) Schematic diagram of one-dimensional index profile in the straight interaction region of fused vertical coupler switches with two sections.

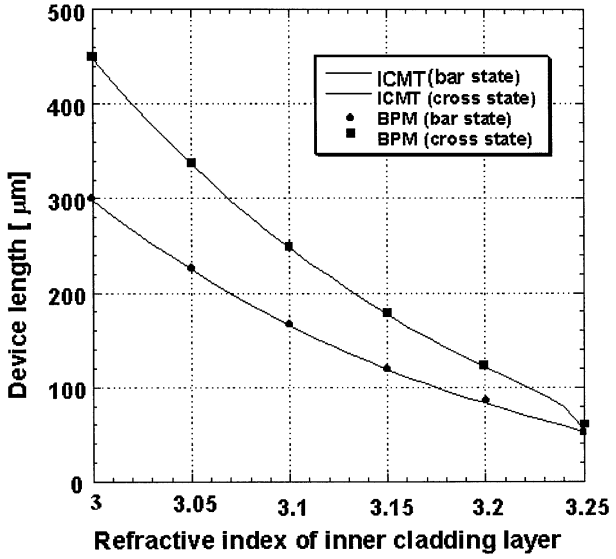

Fig. 2. Device length for bar and cross states with high extinction ratios larger than 30 dB calculated as a function of the refractive index of the inner cladding layer when the inner cladding layer thickness is 0.6 μm.

In order to obtain the design guidelines for ultra short two-section FVCSs, the tolerances of refractive indices of the inner cladding layer and cores which give high extinction ratios larger than 30 dB for three cases denoted in Fig. 3 are calculated. First case is $\Delta n_{ci} = 0.03$, $\Delta n_{\mathrm{asy}} =$ minimum (case I), second case is $\Delta n_{ci} = \Delta n_{\mathrm{asy}} = 0.025$ (case II), and third case is $\Delta n_{\mathrm{asy}} = 0.03$, $\Delta n_{ci} =$ minimum (case III).

Figure 4 shows the refractive index of each layer, device length, and extinction ratios for (a) cross state and (b) bar state when the change of refractive index of the inner cladding layer for the switching operation is 0.03 (case I). The optimum asymmetries of refractive indices of two cores for cross and bar states are $\Delta n_{\mathrm{asy,cross}} = n_{b,\mathrm{cross}} - n_{a,\mathrm{cross}} = 0.021$ and $\Delta n_{\mathrm{asy,bar}} = n_{b,\mathrm{bar}}(1) - n_{a,\mathrm{bar}}(1) = 0.008$, respectively. Since the refractive index of the inner cladding layer for the cross state is larger than that for the bar state, the optimum asymmetry to achieve high extinction ratios for the cross state is larger than that for the bar state. Thus, the limitation of optimum asymmetry is determined by that for the cross state.

In the case of the cross state, the tolerances of refractive indices of the inner cladding layer and cores which give high

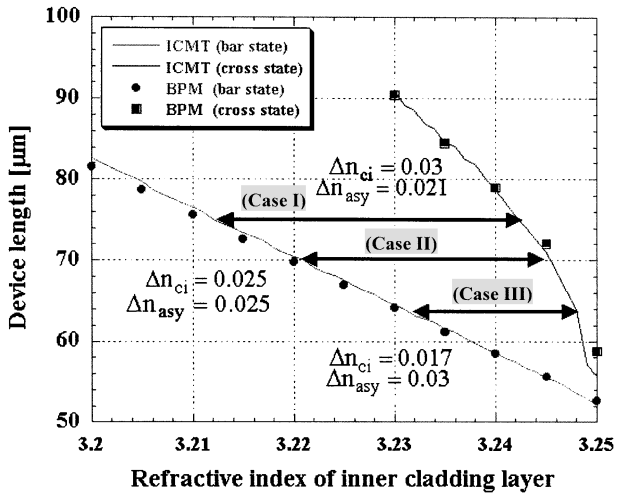

Fig. 3. Detail of Fig. 2 showing the range in the refractive index of the inner cladding layer for the switching operation with the change of refractive indices of the inner cladding layer and cores less than 1% (= 0.03).

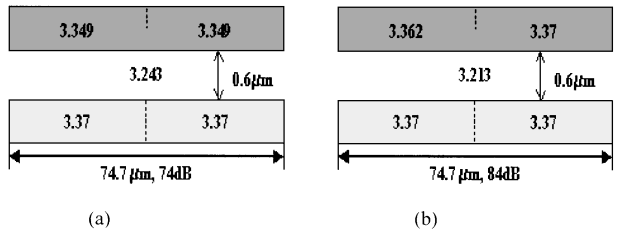

Fig. 4. Refractive index of each layer, device length, and extinction ratio for (a) cross state and (b) bar state when the refractive index change of the inner cladding layer for the switching operation is 0.03 (case I).

extinction ratios larger than 30 dB are $\delta n_{ci}|_{>30\,\mathrm{dB}} = 0.0046$ and $\delta n_{\mathrm{asy}}|_{>30\,\mathrm{dB}=}0.0049$, respectively. In the case of the bar state, the tolerances of refractive indices of the inner cladding layer and cores are $\delta n_{ci}|_{>30\,\mathrm{dB}} = 0.0106$ and $\delta n_{\mathrm{asy}}(1)|_{>30\,\mathrm{dB}} = 0.002$, respectively.

Figure 5 shows the refractive index of each layer, device length, and extinction ratios for (a) cross state and (b) bar state when the change of refractive index of the inner cladding layer and that of cores for the switching operation are the same as 0.025 (case II). Since the optical power confined in cores decreases while that confined in the inner cladding layer increases as the strength of coupling between two cores increases (the refractive index of the inner cladding layer increases), the optimum asymmetry of refractive indices of two cores to obtain the maximum extinction ratio increases while the change of refractive index of the inner cladding layer for the switching operation decreases as the refractive index of the inner cladding layer increases. Thus, the optimum asymmetry of refractive indices of two cores of Fig. 5 is larger than that of Fig. 4. The refractive index change of the inner cladding layer for the switching operation is 0.025 less than that of Fig. 4 (0.03). The optimum asymmetries of refractive indices of two cores for the cross state and the bar state are $\Delta n_{\mathrm{asy,cross}} = n_{b,\mathrm{cross}} - n_{a,\mathrm{cross}} = 0.025$ and $\Delta n_{\mathrm{asy,bar}} = n_{b,\mathrm{bar}}(1) - n_{a,\mathrm{bar}}(1) = 0.009$, respectively.

With the same reason, the tolerance of refractive indices of cores increases while that of the inner cladding layer decreases as the refractive index of the inner cladding layer increases. In the case of the cross state, the tolerance of refractive indices of cores, $\delta n_{\mathrm{asy}}(1)|_{>30\,\mathrm{dB}} = 0.0065$, is larger than that of Fig. 4 (0.0049) while that of the inner cladding layer, $\delta n_{ci}|_{>30\,\mathrm{dB}} = 0.0041$, is smaller than that of Fig. 4 (0.0046). In the case of the bar state, the tolerance of refractive indices of cores, $\delta n_{\mathrm{asy}}(1)|_{>30\,\mathrm{dB}} = 0.0022$, is larger than that of Fig. 4 (0.002) while that of the inner cladding layer, $\delta n_{ci}|_{>30\,\mathrm{dB}} = 0.0092$, is smaller than that of Fig. 4 (0.0106).

Figure 6 shows the refractive index of each layer, device length, and extinction ratios for (a) cross state and (b) bar state when the change of the refractive index of the inner cladding layer for the switching operation is 0.017 (case III). The optimum asymmetries of refractive indices of two cores for the cross state and the bar state are $\Delta n_{\mathrm{asy,cross}} = n_{b,\mathrm{cross}} - n_{a,\mathrm{cross}} = 0.03$ and $\Delta n_{\mathrm{asy,bar}} = n_{b,\mathrm{bar}}(1) - n_{a,\mathrm{bar}}(1) = 0.012$, respectively. Since the case of Fig. 6 is the strongest coupled waveguide system among the three cases considered, the change of the refractive index of the inner cladding layer for the switching operation is the smallest while the optimum asymmetries of refractive indices of two cores for cross and bar states are the largest among the three cases considered. Also, the tolerances of refractive indices of cores for the cross state and bar state, $\delta n_{\mathrm{asy}}(1)|_{>30\,\mathrm{dB}}$, is the largest as 0.014 and 0.0025, respectively, while those of the inner cladding layer, $\delta n_{ci}|_{>30\,\mathrm{dB}}$, are the smallest as 0.0035 and 0.0074, respectively.

Figure 7 shows the device length for the cross state and the bar state with high extinction ratios larger than 30 dB calculated as a function of the refractive index of the inner cladding layer when the inner cladding layer thickness is 0.7 μm. Since the inner cladding layer thickness of Fig. 7 is larger than that of Fig. 3, the coupled waveguide system shown in Fig. 7 is a weaker coupled waveguide system than that shown in Fig. 3 for the same refractive index of the inner cladding layer so that the coupling length of Fig. 7 is longer than that of Fig. 3. Thus, the change of the refractive index of the inner cladding layer for the switching operation increases while the optimum asymmetries of refractive indices of two cores for cross and bar states decrease for the same refractive index of the inner cladding layer as the inner cladding layer thickness increases. For example, the required refractive index change of the inner cladding layer for the switching operation increases from 0.025 to 0.028 and device length increases from 70 μm to 93 μm, while the optimum asymmetries of refractive in-

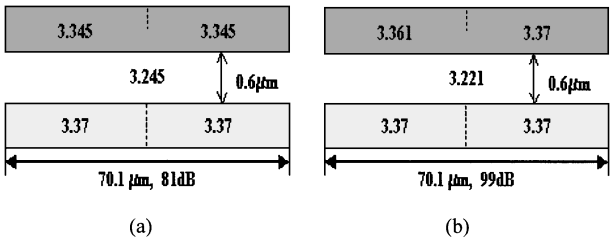

Fig. 5. Refractive index of each layer, device length, and extinction ratio for (a) cross state and (b) bar state when the refractive index change of the inner cladding layer and that of cores for the switching operation are the same as 0.025 (case II).

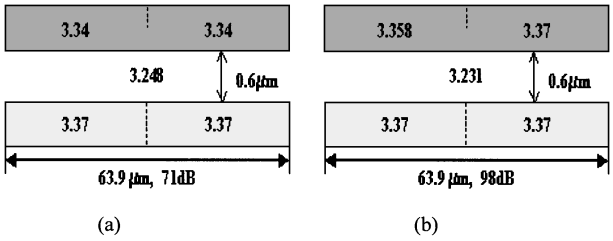

Fig. 6. Refractive index of each layer, device length, and extinction ratio for (a) cross state and (b) bar state when the refractive index change of the core for the switching operation is 0.03 (case III).

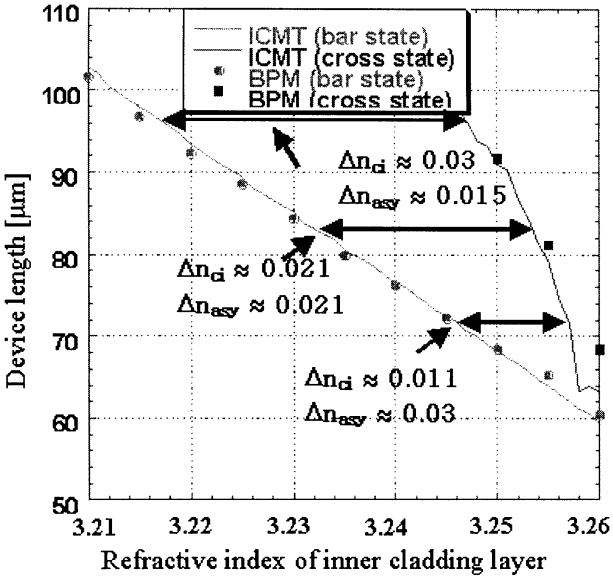

Fig. 7. Device length for bar and cross states with high extinction ratios larger than 30 dB calculated as a function of the refractive index of the inner cladding layer when the inner cladding layer thickness is 0.7 μm.

Table I. Tolerances of refractive indices of the inner cladding layer and cores for the cases in which $\Delta n_{ci} = 0.03$, $\Delta n_{ci} = \Delta n_{\text{asy}}$, and $\Delta n_{\text{asy}} = 0.03$ when the inner cladding layer thickness are 0.5, 0.6, and 0.7 μm, respectively.

	t (μm)	$\Delta n_{ci} = 0.03$ (case I)	$\Delta n_{ci} = \Delta n_{\text{asy}}$ (case II)	$\Delta n_{\text{asy}} = 0.03$ (case III)
$\delta n_{\text{asy}}(1)\|_{>30\,\text{dB}}$	0.5		0.0029	
	0.6	0.0019	0.0021	0.0026
	0.7	0.0015	0.0016	0.0026
$\delta n_{ci}(1)\|_{>30\,\text{dB}}$	0.5		0.0047	
	0.6	0.0046	0.004	0.0035
	0.7	0.0046	0.0037	0.003

dices of two cores for the cross state decrease from 0.025 to 0.016 when the inner cladding layer thickness increases from 0.6 μm to 0.7 μm for the refractive index of the inner cladding layer of 3.22.

In order to investigate the effect of the inner cladding layer thickness on the characteristics of FVCSs, the tolerances are calculated for various thicknesses of the inner cladding layer. The results are shown in Table I. Since refractive indices of the inner cladding layer to achieve the cross state are larger than those of the bar state, the tolerances of refractive indices of the inner cladding layer of the cross state are smaller than those of the bar state, while those of cores of the bar state are smaller than those of the cross state. Thus, we show the small tolerance for each case in Table I.

We can summarize the results as follows:

1. The change of the refractive index of the inner cladding layer for the switching operation and the length of devices decrease as the refractive index of the inner cladding layer increases.
2. The optimum asymmetry of refractive indices of cores for the maximum extinction ratio increases as the refractive index of the inner cladding layer increases.
3. The tolerance $\delta n_{\text{asy}}|_{>30\,\text{dB}}$ increases, while $\delta n_{ci}|_{>30\,\text{dB}}$ decreases as the refractive index of the inner cladding layer increases for the same thickness of the inner cladding layer.
4. The change of the refractive index of the inner cladding layer for the switching operation decreases as the inner cladding layer thickness decreases.
5. The change of the refractive index of cores for the switching operation increases as the inner cladding layer thickness decreases. Thus, there is the minimum thickness of the inner cladding layer for the switching operation if one wants to limit the switching to less than 1% change in refractive indices.
6. The tolerances of refractive indices of cores and that of the inner cladding layer increase as the inner cladding layer thickness decreases.

Design guidelines for ultra short FVCSs are as follows. The tolerances of the refractive index of the inner cladding layer and that of cores increase as the inner cladding layer thickness decreases. The range of the refractive index of the inner cladding layer with its change less than 1% for the switching operation always exists regardless of the inner cladding layer thickness. However, the minimum thickness of the inner cladding layer for the switching operation exists because the change of refractive indices of cores for the switching operation is larger than 1% when the inner cladding layer thickness is less than the minimum thickness. In this case the minimum thickness is 0.5 μm.

It is important to note that achieving large extinction ratios for both cross and bar states requires control of refractive index in both inner cladding and core regions of the waveguides. The required changes can be realized using electro optic effect or carrier injection. With appropriate doping profile and material composition or orientation, one can control the change in the refractive index of different regions. For example Liu *et al.*[5] have recently demonstrated push-pull operation for a vertical coupler switch with a use of a single electrode. This takes advantage of the anisotropic electro-optic effect in zinc-blende semiconductors. In fact when the applied electric field is perpendicular to the (001) surface, it gives a positive index change for TE polarized light propagating along [110] direction and a negative index change for light propagating along the $[1\bar{1}0]$ direction.

4. Conclusions

Both cross and bar states with high extinction ratios larger than 30 dB can be achieved at the same end of ultra short fused vertical directional coupler switches with two sections by changing the refractive indices of the inner cladding layer and cores by an amount less than 1%. The tolerances of the refractive indices of the inner cladding layer and cores to achieve high extinction ratios larger than 30 dB increase as the inner cladding layer thickness decreases. However, the minimum thickness of the inner cladding layer for the switching operation exists because the change of the refractive index of cores for the switching operation is larger than 1% when the inner cladding layer thickness is less than the minimum thickness.

Acknowledgements

This work was supported in part by the Ministry of Information and Communication of Korea "Support Project of University Foundation Research'99" supervised by IITA, by the Korea Science and Engineering Foundation (KOSEF) through the Ultra-Fast Fiber-Optic Networks Research Center at Kwangju Institute of Science and Technology, by the Brain Korea 21 Project in 2001, and by advanced photonics technology.

1) A. Shakouri, B. Liu, B.-G. Kim, P. Abraham, A. W. Jackson, A. C. Gossard and J. E. Bowers: J. Lightwave Technol. **16** (1998) 2236.
2) B.-G. Kim, A. Shakouri, B. Liu and J. E. Bowers: Jpn. J. Appl. Phys. **37** (1998) L930.
3) S.-C. Cho, B.-G. Kim and A. Shakouri: Jpn. J. Appl. Phys. **39** (2000) 6555.
4) S. L. Chuang: *Physics of Optoelectronic Devices* (John Wiley & Sons, New York, 1995) Chap. 8, p. 302.
5) B. Liu, A. Shakouri, P. Abraham and J. E. Bowers: IEEE Photon. Technol. Lett. **11** (1999) 662.